Ferroelectric displacements in multiferroic Y(Mn,Ga)O-3

Adem, U.; Nugroho, A. A.; Meetsma, A.; Palstra, T. T. M.

Published in:
Physical Review. B: Condensed Matter and Materials Physics

DOI:
10.1103/PhysRevB.75.014108

Ferroelectric displacements in multiferroic $Y(Mn,Ga)O_3$

U. Adem,[1] A. A. Nugroho,[1,2] A. Meetsma,[1] and T. T. M. Palstra[1]
[1]*Solid State Chemistry Laboratory, Materials Science Center, University of Groningen, 9747 AG Groningen, The Netherlands*
[2]*Faculty of Mathematics and Natural Sciences, Institut Teknologi Bandung, Jl. Ganesha 10, Bandung 40132, Indonesia*
(Received 31 August 2006; revised manuscript received 26 October 2006; published 11 January 2007)

We have studied the effects of substitution of Mn^{3+} by Ga^{3+} on the crystal structure of $YMnO_3$. $Y(Mn,Ga)O_3$ is a magnetoferroelectric in which the ferroelectric displacements from the YO_7 polyhedra are associated with buckling and tilting of the MnO_5 bipyramids. The differences in ionic radius and orbital occupation between Mn^{3+} and Ga^{3+} result in an increase of the c/a lattice parameter ratio. This dilation is not associated with the displacements of MnO_5 bipyramids, but with the elongation of the YO_6 antiprisms. The magnitude of the local YO_6 dipoles decrease with Ga substitution.

DOI: 10.1103/PhysRevB.75.014108 PACS number(s): 61.10.Nz, 77.80.−e, 77.84.−s

I. INTRODUCTION

$YMnO_3$ is a member of the multiferroic hexagonal manganites family that exhibits both magnetic order ($T_N \sim 75$ K) and reversible spontaneous electric polarization ($T_C \sim 1000$ K). The multiferroic properties are known since the 1960s by pioneering work of Bertaut *et al.*[1] Recently the interaction between the magnetic and ferroelectric state was convincingly shown[2] and much research addresses this coexistence. Much less is known on the origin of the ferroelectric state. A number of high temperature structural studies could not resolve the atomic displacements below T_C from an analysis of the diffraction intensities.[3–5] Recent room temperature (RT) crystallographic studies coupled with band structure calculations showed the relevance of the buckling and tilting of the MnO_5 bipyramids for the stabilization of the ferroelectric state.[5–7] The ferroelectric state is associated with displacements of the oxygen ions that coordinate Y^{3+}, which has formally a d^0-state. The two capping O^{2-} ions of the YO_8 capped trigonal antiprisms displace, yielding a short and a long Y-O bond. The crystal structure of $YMnO_3$ is shown in Fig. 1. It can be considered as stacks of layers of MnO_5 trigonal bipyramids and separated by layers of Y^{3+}. Likewise, it can be constructed from layers of YO_8 capped trigonal antiprisms along c, with the Mn^{3+} located between the capping oxygens. The apical oxygens of the MnO_5 also construct the antiprisms of YO_6, and the planar oxygens of MnO_5 also constitute the caps of the YO_6 antiprisms. The crystal structure can alternatively be constructed from a dense packed anion sublattice. It can be considered to originate from alternating stacks of hexagonal and cubic closed packed oxygen layers. The crystal structure is constructed from *BABCACBAB* stacks of O^{2-}. The Mn^{3+} ions are located in the middle layer of a "hexagonal" *BAB* stack, yielding the bipyramids. The Y^{3+} (or small rare earths) occupy the octahedral holes in a "cubic" *ABCA* stack, where the *B* and *C* layers provide the antiprismatic coordination and the *A* layer the capping oxygens.

The isostructural compounds with the same space group, $P6_3cm$, are reported and predicted to be also ferroelectric (for an overview, see, e.g., Ref. 8). Y can be substituted by small rare earth ions and Mn can be substituted by Ga and In. $YGaO_3$ is one of these isostructural ferroelectric compounds.[9] The replacement of Mn by Ga results both in a change of the orbital occupation (from d^4 to d^{10}) and the ionic radius. The evolution of the structural parameters from $YMnO_3$ to $YGaO_3$ is important and provides a better understanding of the origin of ferroelectricity in these hexagonal systems.

Moreover, while theoretical analysis predicts that the largest local dipole moment and T_C decreases with Ga substitution,[8] recent experimental work showed that T_C increases with Ga substitution.[10] Therefore it is of interest to study the crystallographic response of $YMnO_3$ with Ga substitution. The increase of the c/a lattice parameter ratio with Ga substitution can be associated with decreasing buckling and tilting of MnO_5 bipyramids. We will show that this is not the case but the local coordination of Y1 and Y2 dominates the structural changes.

For conventional perovskite ferroelectrics, the electric dipoles originate in part from the off-center displacement of transition metal cation. This mechanism for ferroelectricity requires formally empty *d*-orbitals.[11] However, for $YMnO_3$

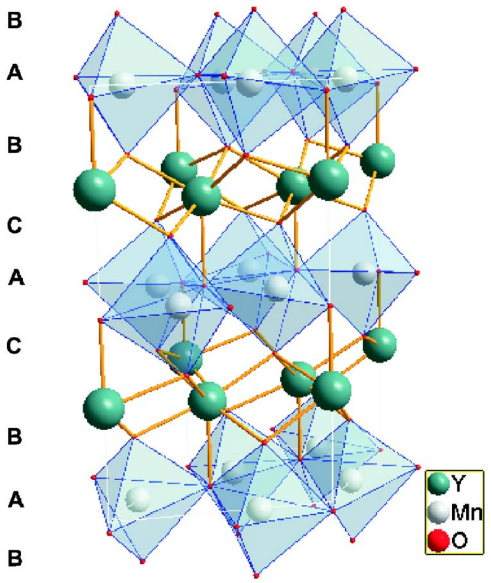

FIG. 1. (Color online) Crystal structure of $YMn_{1-x}Ga_xO_3$ emphasizing the MnO_5 trigonal bipyramids and the mixed hexagonal *BAB* and cubic *ABCA* stacking of the O sublattice.

the *d*-orbital of Mn^{3+} is partially occupied. Therefore the conventional mechanism for ferroelectricity does not apply. It has been shown that the ferroelectricity is associated with the tilting of MnO_5 bipyramids. This tilting away from a planar stacking results in oxygen displacements along the stacking direction (*c*-axis). These displacements result in the differentiation of the capping oxygens of the YO_8 polyhedra, as two out of three of the capping oxygens "move" up and the other "move" down along the *c*-axis.

Mn substitution by Ga is expected to have two effects. First, the doubly occupied d_{z^2} orbital in Ga is expected to expand the apical Mn–O bond, which should decrease the tilting and thus the dipole moments. Second, the smaller ionic radius of Ga^{3+} compared with Mn^{3+} should also result in a smaller tilting. We will show that this is not the case and that the antiprismatic oxygens, coordinating Y^{3+}, contribute significantly to the dipole formation. We provide structural data for $YMn_{1-x}Ga_xO_3$ for $x=0$, 0.1, 0.3, and 0.5 at 100 K. We use literature data of $YMnO_3$ (Ref. 12) and $YGaO_3$ (Ref. 9) at RT as reference.

II. EXPERIMENT

$YMn_{1-x}Ga_xO_3$ ($x=0$, 0.1, 0.3, and 0.5) crystals were grown by a floating zone furnace (Crystal Systems Inc.). The oxygen partial pressure was increased with increasing Ga concentration in order to stabilize the molten zone. The crystals have a 5 mm diameter and are a few cm long. Single crystal diffraction experiments were carried out on selected small chipped off pieces. We used a Bruker SMART APEX charge coupled device diffractometer with graphite monochromated Mo $K\alpha$ radiation and cooled the crystal to 100 K. The SHELXL software package was used for the refinement.[13] Values of R_{wp} for refinement are 0.0797, 0.1939, 0.1448, and 0.0973 for $x=0$, 0.1, 0.3, and 0.5, respectively. Corresponding R_F values for the respective compositions were 0.0314, 0.0877, 0.0605, and 0.0342. Goodness of the fit was typically close to 1. The refinements included not only the structural parameters but also the site occupancy. The refinements indicated full occupation of the Y and O sites, but deviations were observed for the (Mn,Ga) occupation from the nominal values. Nevertheless, we use in our analysis the nominal composition. The room temperature refinements used for reference were obtained on Bi_2O_3 flux grown $YMnO_3$ crystals.[12] The structural parameters of $YGaO_3$ were taken from Geller *et al.*[9] The polycrystalline $YGaO_3$ sample was synthesized by inductive melting and the diffraction data was collected at RT. For the calculation of the lattice parameters, single crystal samples were crushed and powder diffraction was done. The diffraction data was refined using the software package GSAS.[14] All of the other structural parameters were calculated from the single crystal diffraction results.

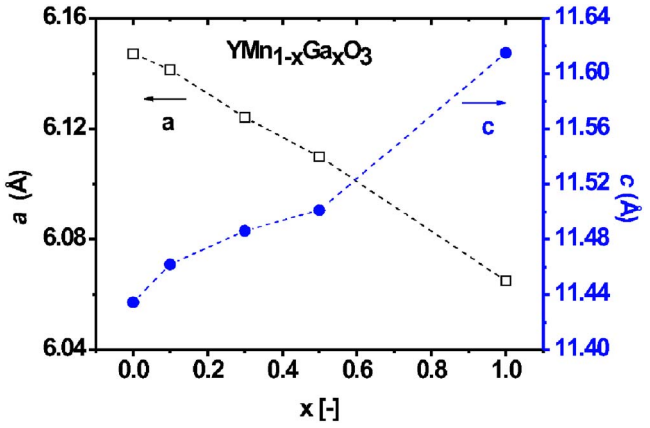

FIG. 2. (Color online) Lattice parameters, *a* and *c*, of $YMn_{1-x}Ga_xO_3$ at room temperature from powder diffraction.

III. RESULTS AND DISCUSSION

In previous work, we investigated the role of the rare earth ion on the structural parameters.[15] We showed that for smaller R^{3+} ionic radius the tilting and buckling of the structure increases leading to larger local dipole moments. Here, we focus on the role of the *B*-site. Ga^{3+} has a smaller ionic radius than Mn^{3+}, caused by the larger nuclear charge. Second, Ga^{3+} has a d^{10} configuration, contrasting the d^4 configuration of Mn^{3+}. We note that Mn^{3+} is not Jahn-Teller active in a trigonal bipyramidal coordination, as the highest d_{z^2} level is nondegenerate.[16] The ground states are d_{xz} and d_{yz}, followed by degenerate d_{xy} and $d_{x^2-y^2}$ at an intermediate energy level.

Figure 2 shows the lattice parameters for $YMn_{1-x}Ga_xO_3$. The lattice parameters change roughly linearly from $YMnO_3$ to $YGaO_3$, obeying Vegard's law. The decrease in the lattice parameter *a* can be explained by the smaller ionic radius of Ga. The increase in the *c*-axis would according to the considerations above, be ascribed to the filling of the d_{z^2} antibonding orbitals. Below, we will show that this is not the

TABLE I. Mn–O bond distances for $YMn_{1-x}Ga_xO_3$ at 100 K obtained from single crystal diffraction refinements and at 293 K for $x=0$ (from Ref. 12) and from powder diffraction refinement at 293 K (from Ref. 9).

x	0 (from Ref. 12)	0	0.1	0.3	0.5	1.0 (from Ref. 9)
Mn–O1	1.858(7)	1.8610(7)	1.915(16)	1.866(12)	1.851(9)	1.8403(17)
Mn–O2	1.876(7)	1.8950(7)	1.852(17)	1.875(12)	1.903(12)	1.8416(17)
Mn–O3	2.054(3)	2.0790(2)	2.086(5)	2.060(4)	2.062(4)	2.0563(11)
Mn–O4	2.062(2)	2.0494(12)	2.053(3)	2.047(3)	2.0406(18)	2.0172(9)

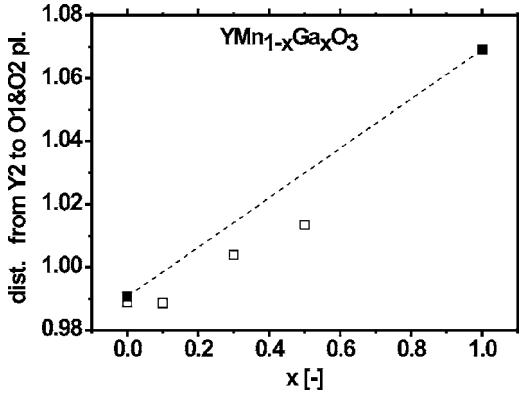

FIG. 3. Average distance of Y1 (Y2) to O1 and O2 planes vs Ga concentration. Filled squares denote the data at 293 K, unfilled ones denote the data at 100 K. The line is a guide to the eye.

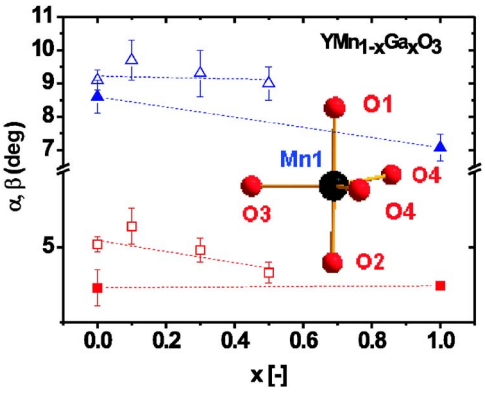

FIG. 4. (Color online) Tilting angle α and buckling angle β vs Ga concentration. Squares denote α and triangles denote β. Filled symbols denote the values at 293 K, whereas unfilled ones denote values at 100 K.

case, and that the local Y-coordination is responsible for the structural changes.

In Table I we show the Mn–O bond lengths. The apical Mn–O bond lengths (Mn–O1 and Mn–O2) are significantly smaller than the planar Mn–O3 and Mn–O4 bond lengths. Our structural data indicate that the apical Mn–O distances do not change upon Ga substitution, at least not proportionally with the lattice parameter c. Occupying the antibonding d_{z^2} orbital has no noticeable effect on the apical Mn–O bond length.

In contrast, the Y-coordination does change. In Fig. 3 we show the average distance of Y to the coordinating O1 and O2 planes. By symmetry the O1 ions have the same z-coordinate and the same is true for the O2. The O1 (O2) ions are thus located in a plane perpendicular to the c-axis. The averaged distance of Y1 (Y2) to the O1 and O2 planes increases by 6% upon substitution of Mn^{3+} by Ga^{3+}. This indicates a strong elongation of the YO_6 antiprism. Therefore the c lattice parameter expansion upon the substitution of Mn^{3+} by Ga^{3+} is not caused by the change in local coordination of Mn^{3+}, but by the change in the local coordination of Y^{3+}. Likewise, the substitution also does not significantly change the planar Mn–O3 and Mn–O4 distances, nor the O1–O1 and O2–O2 distances coordinating Y^{3+}. This suggests that the changes in crystal structure are strongly associated with the coordination changes of Y^{3+}.

We parametrize the tilting angle, α, by the angle of the apical O1–O2 axis of a MnO_5 bipyramid with the c-axis. The buckling is defined by the angle β of the plane spanned by the base of the MnO_5 bipyramid, the O4–O4–O3 plane, with the c-axis. The changes in the angles α and β are shown in Fig. 4. While the error bars are substantial, the data indicate that the tilting and buckling of the MnO_5 bipyramids do not change substantially upon Ga-substitution. This contrasts with the substitution in the A-site, where the tilting angle α decreases by 17% per about 4% increase in ionic radius (for R=Y, Yb, and Lu).

We can now relate these changes of the crystal structure with the changes in the local dipole moments. Similar to $YMnO_3$, upon Ga substitution, Ga remains in the barycenter of the bipyramids. Previously, we emphasized that the local dipoles originate from the unequal displacement of the cap oxygen ions of the YO_6 antiprisms. One cap O3 (O4) has almost the same distance to Y1 (Y2) as the antiprism oxygens ~2.3 Å, which corresponds to the sum of the ionic radii of Y^{3+} and O^{2-}. However, the other cap oxygen is approximately 1 Å further away. We note that the local dipole originates nevertheless mostly from noncentered antiprismatic coordination of Y^{3+} and only to a lesser extent from the cap oxygens. In Fig. 5 we show the local dipole, Y1 resulting from the $Y1O_6$ antiprism and $Y1O_8$ capped antiprisms. The local dipole moment was calculated as the distance from the center of gravity of 6 (8) oxygens, to the Y1. Clearly, the local Y1 dipole decreases upon Ga-substitution. The small difference between the local dipoles resulting from $Y1O_6$ and $Y1O_8$ indicates that the dipoles originate mostly from the antiprismatic coordination.

While our structural studies indicate that Ga substitution decreases the local dipole moments, the effect on the polarization is less clear. The polarization should take into account that the multiplicity of the Y2-site is twice that of the Y1-site. Substraction of the antiparallel displacements with ap-

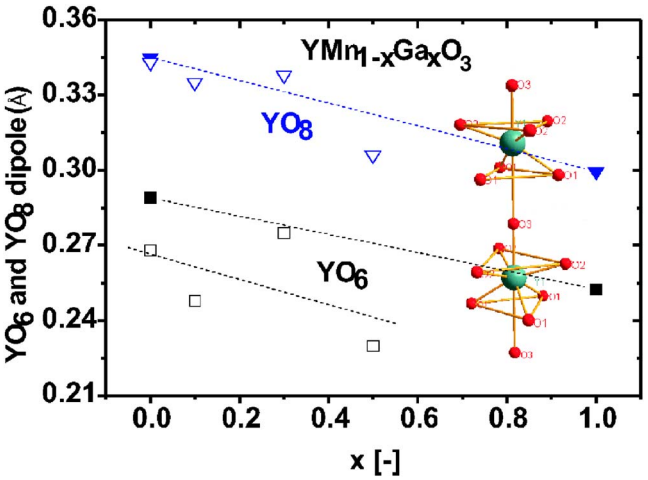

FIG. 5. (Color online) Local dipole Y1, arising from Y1O6 and Y1O8 capped antiprisms for $YMn_{1-x}Ga_xO_3$. Squares denote $Y1O_6$ dipoles and triangles denote $Y1O_8$ dipoles. Filled symbols denote the values at 293 K, whereas unfilled ones denote values at 100 K.

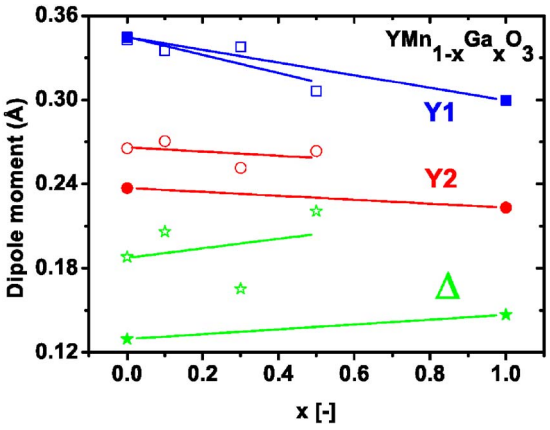

FIG. 6. (Color online) Dipole moments Y1, Y2, and △ (2Y2-Y1) for $YMn_{1-x}Ga_xO_3$ as defined in the text. Squares denote Y1 dipoles, circles Y2, and stars denote △. Filled symbols denote the values at 293 K, whereas unfilled ones denote values at 100 K.

propriate multiplicity reveals no clear change of the total dipole upon Ga substitution (see Fig. 6). Abrahams associates the ferroelectric transition temperature with the magnitude of the largest local dipole.[8] This approach predicts a reduction of the ferroelectric transition temperature with Ga substitution: from 1220 K for $x=0$ to 1020 K for $x=1$. In contrast, Zhou *et al.* report an increase of the ferroelectric transition temperature: from 900 K for $YMnO_3$ to 925 K for $YMn_{0.8}Ga_{0.2}O_3$.[10] This indicates that the coupling between the local dipoles is also important to understand the structural effects associated with Ga substitution. The small changes in the crystal structure with Ga substitution contrast with very large changes in the magnetoelectric coupling.[17]

IV. CONCLUSIONS

We have studied the structural response of single crystal $YMnO_3$ upon substitution of Mn^{3+} by Ga^{3+}. Ga^{3+} substitution decreases the lattice parameter a, and increases c. The smaller ionic radius and filled d_{z^2} orbital were expected to change the local coordination around the Mn-site. This was not the case. In contrast, we observe a much larger response in the coordination of the Y-site. Ga substitution results in an elongation of the YO_6 antiprisms, in which the Y-ions become more closely located near the barycenter. Despite the decrease in the local dipoles, the total polarization does not decrease markedly because of the antiparallel displacements of the $Y1O_6$ and $Y2O_6$ local dipoles. These results contrast Y-substitution by smaller rare earth R-ions. Here, a smaller R results in an increased tilting and buckling. The substitution of Mn^{3+} by Ga^{3+} does not increase the tilting and buckling.

ACKNOWLEDGMENTS

We acknowledge stimulating discussions with G. Nénert, N. Mufti, and G. R. Blake; we thank J. Baas for the technical support. This work was supported by the "Stichting voor Fundamenteel Onderzoek der Materie" (FOM). The work of A.A. Nugroho was supported by the NWO Breedtestrategie Program of the Material Science Center, RuG and by KNAW, Dutch Royal Academy of Sciences, through the SPIN program.

[1] E. F. Bertaut, F. Forrat, and P. Fang, Compt. Rend. **256**, 1958 (1963).
[2] M. Fiebig, T. Lottermoser, D. Frohlich, A. V. Goitsev, and R. Pisarev, Nature (London) **499**, 6909 (2002).
[3] T. Katsufuji, M. Masaki, A. Machida, M. Moritomo, K. Kato, E. Nishibori, M. Takata, M. Sakata, K. Ohoyama, K. Kitazawa, and H. Takagi, Phys. Rev. B **66**, 134434 (2002).
[4] T. Lonkai, D. G. Tomuta, U. Amann, J. Ihringer, R. W. Hendrikx, D. M. Tobbens, and J. A. Mydosh, Phys. Rev. B **69**, 134108 (2004).
[5] G. Nénert, M. Pollet, S. Marinel, Y. Ren, A. Meetsma, and T. T. M. Palstra, cond-mat/0601547 (to be published); G. Nénert, Y. Ren, H. T. Stokes, and T. T. M. Palstra, cond-mat/0504546 (to be published).
[6] B. B. van Aken, T. T. M. Palstra, A. Filippetti, and N. A. Spaldin, Nat. Mater. **3**, 164 (2004).
[7] C. J. Fennie and K. M. Rabe, Phys. Rev. B **72**, 100103(R) (2005).
[8] S. C. Abrahams, Acta Crystallogr., Sect. B: Struct. Sci. **B57**, 485 (2001).
[9] S. Geller, J. B. Jeffries, and P. J. Curlander, Acta Crystallogr., Sect. B: Struct. Crystallogr. Cryst. Chem. **B31**, 2770 (1975).
[10] H. D. Zhou, J. C. Denyszyn, and J. B. Goodenough, Phys. Rev. B **72**, 224401 (2005).
[11] N. A. Hill, J. Phys. Chem. B **104**, 6694 (2000).
[12] B. B. van Aken, A. Meetsma, and T. T. M. Palstra, Acta Crystallogr., Sect. C: Cryst. Struct. Commun. **C57**, 230 (2001).
[13] G. M. Sheldrick, SHELXL-97, Program for the Refinement of the Crystal Structures, University of Göttingen, Germany, 1997.
[14] A. C. Larson and R. B. Von Dreele, Los Alamos National Laboratory Report No. LAUR 86–748, 2000 (unpublished).
[15] B. B. Van Aken and T. T. M. Palstra, Phys. Rev. B **69**, 134113 (2004).
[16] B. B. Van Aken, Jan-Willem G. Bos, R. A. de Groot, and T. T. M. Palstra, Phys. Rev. B **63**, 125127 (2001).
[17] A. A. Nugroho, U. Adem, M. O. Tija, M. Mostovoy, and T. T. M. Palstra (unpublished).